

Preequilibrium model analysis of (p,n) reactions on isotopes of Zr and Mo

Isao Kumabe and Yukinobu Watanabe

Department of Nuclear Engineering, Kyushu University, Fukuoka 812, Japan

(Received 27 March 1987)

The neutron energy spectra from the (p,n) reaction on $^{90,91,92,94}\text{Zr}$, $^{92,94,95,96,97,98,100}\text{Mo}$, and ^{110}Pd with 25 MeV protons and $^{90,91,92,94}\text{Zr}$ with 18 MeV protons are analyzed in terms of the preequilibrium exciton model introducing effective Q values, the pairing correlation, and the modified uniform spacing model in which the uniform spacing model is modified so as to have a wide spacing at the magic number. For all these targets, the calculated spectra using the above model for 25 MeV protons show good agreement with the experimental ones not only on the absolute cross sections in the neutron energy region of 12–18 MeV, but also on the observed spectra with pronounced structures in the neutron energy region higher than 18 MeV.

I. INTRODUCTION

Scobel *et al.*^{1,2} have reported the energy spectra of neutrons emitted from the (p,n) reactions on $^{90,91,92,94}\text{Zr}$, $^{92,94,95,96,97,98,100}\text{Mo}$, and ^{110}Pd at 25 MeV and from those on $^{90,91,92,94}\text{Zr}$ at 18 MeV in order to study the shell and odd-even effects in the preequilibrium process. In the high neutron energy region of the spectra, pronounced structures arising from the shell closure were observed in the neutron spectra for magic and near magic nuclei (^{90}Zr , ^{91}Zr , ^{92}Zr , ^{92}Mo , and ^{94}Mo). These pronounced structures were qualitatively explained¹ on the basis of proton-particle neutron-hole state densities generated from different sets of single particle states using the recursion method by Williams *et al.*³

Scobel *et al.*¹ have also analyzed the neutron spectra from $^{90,91,92,94}\text{Zr}$ (p,n) reactions using the geometry-dependent hybrid model plus evaporation model. The calculated cross sections for $^{91,92,94}\text{Zr}$ were too large as compared with the experimental ones, though fairly good agreement was obtained for ^{90}Zr . On the other hand, it is seen from inspection of the experimental 25 MeV (p,n) spectra^{1,2} for Zr isotopes, that the cross sections in the 12–18 MeV region of the emitted neutron energy increase smoothly with increasing mass number. Namely, the shell irregularities observed in the high neutron energy region disappear in the 12–18 MeV region.

The shape and magnitude of spectra calculated with the preequilibrium model depend on mainly the state density used in the model. A formula given by Williams⁴ has widely been employed as the particle-hole state density. This formula is based on the uniform spacing model and is expressed as a function of the single particle level density g and the excitation energy. For the (p,n) reaction, the excitation energy of the residual nucleus and that of the composite nucleus are connected with the reaction Q value $Q(p,n)$ and the proton binding energy B_p , respectively, because the former is given by $E_p - E_n + Q(p,n)$, where E_p is the incident proton energy and E_n the emitted neutron energy, and the latter is equal to $E_p + B_p$.

In general, it is known that the nuclear shell effect appears obviously in the values of $Q(p,n)$ and B_p near the shell closure and the large variations associated with the

pairing energy effect are also exhibited. This indicates that the shell effect is implicitly introduced in the preequilibrium calculation through two quantities $Q(p,n)$ and B_p , even though shell independent g is used. Hence the use of shell-independent values for $Q(p,n)$ and B_p is preferable to reproduce the measured spectra in the 12–18 MeV region by the preequilibrium calculation using the state density of Williams.⁴

On the other hand, one of the authors⁵ has analyzed the measured cross sections of the 14 MeV (n,p) reaction, which is the inverse reaction of the (p,n) reaction, for nuclei with mass number larger than 90 in terms of the preequilibrium exciton model using the effective Q values, which are derived from a semiempirical mass formula whose parameters are smooth functions of mass number and are free from fluctuations near closed shells. By introducing the effective Q value instead of the true Q value in the exciton model, the ratios of experimental and theoretical cross sections approached 1.0; their derivations from 1.0 were markedly ameliorated.

In the present study, therefore, we introduce the effective Q values in the analysis of the (p,n) reaction measured by Scobel *et al.*^{1,2} First the effective Q values for the (p,n) reaction and the effective proton binding energies are derived in Sec. II A. Then the effective Q value and the effective proton binding energy are used to analyze the neutron energy spectra in the continuum region corresponding to intermediate excitation energies (Sec. III). Next, since the uniform spacing model does not include the shell effect, we modify the uniform spacing model so as to have a wide spacing at the magic number (Secs. II B and II C). Moreover, the pairing correlations are taken into account (Sec. II D). The effective Q values introduced by us are discussed in relation to the modification of the state densities (Sec. III). Our conclusions are given in Sec. IV.

II. THEORETICAL CONSIDERATION

A. Effective Q value and effective proton binding energy

The effective Q value⁵ for the (n,p) reaction is expressed as

$$Q = (M_n - M_H)C^2 + b(Z - Z_0 - \frac{1}{2}) \quad (\text{MeV}), \quad (1)$$

where M_n and M_H are the masses of the neutron and hydrogen atom, respectively, and Z is the atomic number of the target nucleus. The values of Z_0 and b are expressed as

$$Z_0 = -0.0001838 A^2 + 0.4255 A + 2.372, \quad (2)$$

$$b = 0.0001008 A^2 - 0.03728 A + 4.678, \quad (3)$$

where A is the mass number of the target nucleus. The effective Q value for the (p,n) reaction is easily derived from that for the (n,p) reaction. The effective Q value for the (p,n) reaction is expressed as

$$Q = -\{(M_n - M_H)C^2 + b[(Z + 1) - Z_0 - \frac{1}{2}]\} \quad (\text{MeV}). \quad (4)$$

The expression of energy spectra in the preequilibrium exciton model includes the excitation energy of a composite nucleus which is calculated from the incident particle energy and the binding energy of its particle in the composite nucleus [for example, see Eq. (1) in Ref. 6]. Inspection of proton binding energy compiled by Wapstra *et al.*⁷ leads to the fact that the nuclear shell effect is obviously exhibited in the proton binding energies near a closed shell. If we use the effective Q value in the preequilibrium model calculation for (p,n) reactions, it is also necessary to use the proton binding energy which has no shell effect; this proton binding energy is referred to as the effective proton binding energy from now on.

The effective proton binding energy was calculated in a manner similar to the calculation of the effective Q value. True proton binding energies for a given atomic number increase almost linearly with the mass number. Therefore, the approximate value of the true proton binding energy can be estimated using the parameters A_0 and B chosen so as to fit proton binding energies of adjacent isotopes by a straight line, where A_0 is the mass number at the point where the straight line intersects with the 6.0 MeV line and B the slope of the line. The approximate proton binding energy, therefore, is expressed as

$$B_p = B(A - A_0) + 6.0, \quad (5)$$

where A is the mass number of the target nucleus.

The values of A_0 and B for each atomic number Z can be determined from the least squares analysis of corresponding isotopes. The Z dependence of both A_0 and B seems to have some remaining structures near closed shells. In order to obtain shell-independent values of A_0 and B , we have fitted the values of A_0 and B by the least squares procedure using quadratic functions of Z . As a result the smoothed values of A_0 and B are

$$A_0 = 0.0062Z^2 + 2.049Z - 2.620, \quad (6)$$

$$B = 0.00035Z^2 - 0.0453Z + 1.723. \quad (7)$$

From Eqs. (5)–(7) the effective proton binding energy can be easily calculated as functions of A and Z . The effective neutron binding energy has been used in the analysis of the (n,p) reaction although it has not been written explicitly in the previous paper.⁵

B. Modification of uniform spacing model

It has been well known that large energy jumps of orbit spacings occur at the magic number in the usually adopted shell model with spin-orbit coupling as shown in Fig. 1(a). However, the uniform spacing model as shown in Fig. 1(c) is often used^{4,6} in the preequilibrium model, although it does not include the shell effect. In order to take the effect of the shell gap into account, therefore, we modified the single particle levels based on the uniform spacing model so as to have a wide spacing at the magic number, as shown in Fig. 1(b). The energy gap at the magic number $N = 50$ shown in Fig. 1(b) was chosen to be nearly equal to the energy gap between $1g_{9/2}$ and $2d_{5/2}$ states.

The leading term in preequilibrium spectra is particle emissions from exciton number $n = 3$ states in the composite nucleus. For example, the contribution from $n \geq 5$ was calculated to be only about 15% in the energy region larger than 12 MeV of the neutron energy in the preequilibrium calculation for the 25-MeV $^{94}\text{Mo}(p,n)$ reaction. In the preequilibrium model the energy spectrum from $n = 3$ states is proportional to the density of $n = 2$ states in the residual nucleus in first order; these states correspond to one proton-particle and one neutron-hole $[(1p)(1n)^{-1}]$ states for (p,n) reactions. In Sec. II C we will describe the procedure to derive the density of $(1p)(1n)^{-1}$ states from two sets of single particle level schemes; one is based on the uniform spacing model widely used in the preequilibrium model, and the other is based on the modified uniform spacing model mentioned in this subsection. Therefore, energy spectra were calculated using the level densities obtained from the modified uniform spacing model for only $n = 3$ and the level densities obtained from

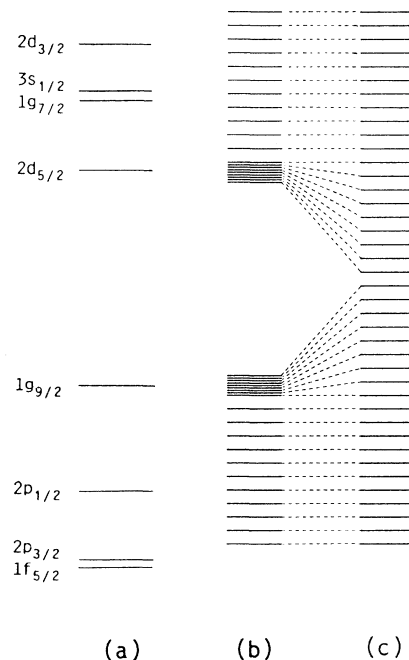


FIG. 1. (a) Shell model with spin-orbit coupling; (b) modified uniform spacing model; (c) uniform spacing model.

the uniform spacing model for $n \geq 5$ for the sake of simplicity.

C. Level density of residual nuclei

In the case of the neutron emission from states of $n = 3$ in the (p,n) reaction, an incident proton is captured in one of the unoccupied orbits and an outgoing neutron is emitted from one of the occupied orbits.

Firstly, in the uniform spacing model we consider the excited states of the residual nucleus formed by the combination of neutron hole states [*B* in Fig. 2(a)] and proton particle states [*A* in Fig. 2(a)]. If neutrons and protons are filled up to orbits *a* and *a'*, respectively, the one-particle one-hole states excited by the (p,n) reaction are formed in the following manner. When a neutron is emitted from the orbit *a* and a proton is captured in the orbit *b'*, *c'*, *d'*, etc., the excited states are formed as shown in the first row *a* in Fig. 2(b). In the case of the combination of the orbit *b* and the orbits *b'*, *c'*, *d'*, etc., the excited states are formed as shown in the second row *b* in Fig. 2(b), where uniform spacing excited states other than the first row *a* in Fig. 2(b) is represented only by the frame in order to simplify the figure. Consequently, as shown in Fig. 2(b), the level density is linearly proportional to the excitation energy, because the number of the excited states per unit energy interval ΔU as a function of the excitation energy *U* is equal to the level density. This is an ordinary shell-independent case.

Secondly, we consider the excited states of the residual nucleus formed by the combination of neutron hole states [*C* in Fig. 2(a) using the modified uniform spacing model] and proton particle states [*A* in Fig. 2(a) using the uniform spacing model]. If neutrons and protons are filled up to orbits *a* and *a'*, respectively, the states excited by the neutron emission from states of $n = 3$ are formed in the similar manner to the previous case and are shown in Fig. 2(c).

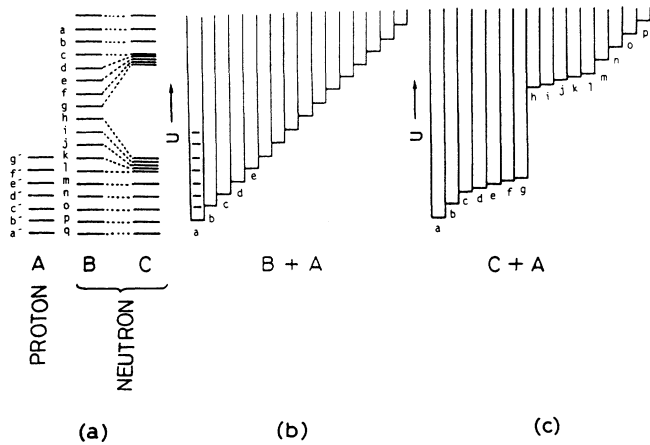


FIG. 2. (a) Uniform spacing model and modified uniform spacing model (simplification of the models in Fig. 1); (b) excited states of the residual nuclei formed by the combination of neutron hole states *B* and proton particle states *A*; (c) excited states of the residual nuclei formed by the combination of neutron hole states *C* and proton particle states *A*.

In the case of magic nuclei such as ^{90}Zr and ^{92}Mo , neutrons are filled up to the orbit *h* in the modified uniform spacing model *C* in Fig. 2(a). Therefore, the excited states start from *h* in Fig. 2(c). In the case of the near magic nuclei with a few neutrons outside of the magic shell such as ^{94}Mo or ^{96}Mo , neutrons are filled up to the orbit *g* or *f*. Therefore, the excited states start from *g* or *f* in Fig. 2(c).

The level densities of the residual nuclei for states of $n = 2$ in the (p,n) reactions on ^{90}Zr , ^{92}Zr , and ^{94}Zr , obtained from the modified uniform spacing model are shown schematically by the solid curves in Figs. 3(a)–(c) as a function of the excitation energy *U*. The effect of the shell gap introduced in the modified uniform spacing model appears in the low excitation region for near shell closure nuclei, while this effect disappears in the intermediate excitation region.

As described above, the level density obtained from the uniform spacing model is represented by a straight line. If the true *Q* values and the uniform spacing model are used in the preequilibrium calculation, the level densities are shown by dotted curves having the origins at *G* which correspond to the true ground states. These curves deviate largely from the solid curves as shown in Figs. 3(a)–(c).

On the other hand, if the effective *Q* values and the uni-

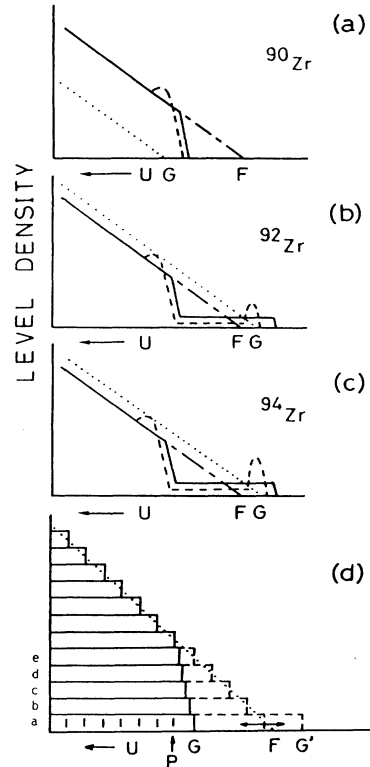


FIG. 3. Schematic level densities at the residual nuclei from the (p,n) reaction on ^{90}Zr , ^{92}Zr , and ^{94}Zr calculated with various models. [Dotted curves: uniform spacing (US) model using true *Q* values, dotted-dashed curves: US model using the effective *Q* values (Q_e), solid curves: modified uniform spacing (MUS) model using Q_e , and dashed curves: MUS model using Q_e plus pairing correlation.]

form spacing model are used, the level densities are represented by dotted-dashed curves having the origins at F which correspond to the fictitious ground states related with the effective Q values. These curves coincide with the solid curves except for the low excitation energies. In other words, it can be understood from Fig. 3(d) that the level density in the excitation energy region higher than the point P is not affected at all by the shift to the left or the right of the frames a , b , c , d , and e . Therefore, in the intermediate excitation region, the use of the uniform spacing model with the effective Q value is equivalent to the use of the modified uniform spacing model.

D. Pairing correlation

In the derivation of the density of $(1p)(1n)^{-1}$ states from single particle levels based on the modified uniform spacing model as mentioned above, the pairing correlation are not taken into account.

If the pairing correlations are taken into account, the excitation energy of two-quasiparticle state is given by

$$U = [(\epsilon_p - \lambda_p)^2 + \Delta_p^2]^{1/2} + [(\epsilon_n - \lambda_n)^2 + \Delta_n^2]^{1/2}, \quad (8)$$

where ϵ is the single particle energy, λ the Fermi energy, and Δ the energy gap. Subscripts p and n mean proton and neutron shells, respectively. Here Δ_n or Δ_p is seen to represent⁸ the odd-even mass difference which is the so called "pairing energy." Therefore we assume that Δ_n or Δ_p is equal to the corresponding pairing energy. The level densities calculated by using the modified uniform spacing model, the effective Q value and Eq. (8) are shown schematically by dashed curves in Figs. 3(a)–3(c). The peak structures shown in Figs. 3(a)–(c) arise from a condensation of excited states by transformation of a single particle level into a quasiparticle level.

III. ANALYSIS AND DISCUSSION

For (p,n) reactions on nuclei with a given atomic number the cross sections calculated with the preequilibrium exciton model increase with increasing Q value. It is seen from an inspection of the experimental 25 MeV (p,n) spectra^{1,2} for Zr isotopes that the cross sections in 12–18 MeV region of the emitted neutron energy increase smoothly with increasing mass number, in spite of large difference of the true Q values between the magic nucleus ^{90}Zr and ^{92}Zr and that between the even-even nucleus ^{92}Zr and the odd nucleus ^{91}Zr . This experimental trend is expected to be reproduced by the preequilibrium cross sections calculated by using the effective Q value which is a smooth function of mass number for a given atomic number.

In the present analysis we used the computer code PREANG (Ref. 9) which calculates emission spectra and angular distribution of particles emitted in the preequilibrium nuclear reaction. The calculations were carried out with the use of the test option to simulate the closed-form preequilibrium model⁹ by setting the transition rates $\lambda_{n \rightarrow n-2} = 0$ and $\lambda_{n \rightarrow n} = 0$, where n was limited to $\bar{n} = \sqrt{2gE}$. The reaction cross sections for protons were calculated from the optical model with the parameters obtained by Mani *et al.*,¹⁰ while those for neutrons were taken from the diagrams presented by Lindner¹¹ using the

nonlocal optical potential by Perey and Back. The square value of the empirical effective matrix element is expressed by the relation $M^2 = KA^{-3}E^{-1}$,¹² where A is the mass number and E is the excitation energy of the composite nucleus.

First, we show the comparisons of the experimental spectra and the calculated ones with the true Q value and with the effective Q value, within the framework of the exciton model with the particle-hole state density formula by Williams.⁴ In these calculations the single particle level density $g = A/13$ was used.

The experimental angle-integrated energy spectra for Zr isotopes^{1,2} are shown by the histograms in Fig. 4. The energy spectra calculated using the true Q values and the uniform spacing model are shown by dotted-dashed curves in Fig. 4. It can be seen from these figures that the calculated spectra for ^{92}Zr and ^{94}Zr show fairly good agreement with the experimental ones except for the neutron energy higher than 18 MeV, but too small values for ^{90}Zr and large values for ^{91}Zr are given.

The energy spectra calculated using the effective Q values and the uniform spacing model are also shown by solid curves in Fig. 4. The calculated spectra show good agreement with the experimental ones for all the targets shown except for $E_n > 18$ MeV. In both calculations the K value was chosen to be 390 MeV.³

As mentioned above, the energy spectra calculated using the effective Q values and the uniform spacing model show good agreement with the experimental ones for all targets except for high neutron energy region. As seen in Fig. 4, the contribution of the cross section in the high neutron energy region is rather small for the total cross section. Therefore, this fact can qualitatively explain that the deviations from 1.0 of the ratios of experimental total (n,p) cross sections to theoretical ones calculated using the effective Q values were markedly reduced⁵ as compared with the use of the true Q values.

Next, we calculated the energy spectra by using the effective Q values, the modified uniform spacing model, and the pairing correlation. Since the neutron emission from $n = 3$ states is dominant at the neutron energy region of interest, more realistic state densities based on the modified uniform spacing model were used in order to describe only the density of $(1p)(1n)^{-1}$ states of the residual nucleus after $n = 3$ emission as a first approximation. For the other state densities, Williams formula derived from the uniform spacing model was employed. The energy gap at the magic number $N = 50$ shown in Fig. 1(b) was chosen to be 4.2 MeV which was nearly equal to the energy gap between $1g_{9/2}$ and $2d_{5/2}$ states. The uniform spacing shown in Fig. 1(c) is 0.275 MeV which was deduced from the level density $g_N = A/(13 \times 2)$ and mass number $A = 95$. The pairing energies in Eq. (8) were chosen so as to obtain the overall good agreement with the peak energies in the experimental energy spectra. $\Delta_n = 0.85$ MeV and $\Delta_p = 1.3$ MeV were used for Zr isotopes and ^{110}Pd , and $\Delta_n = 0.8$ MeV and $\Delta_p = 0.9$ MeV for Mo isotopes. Although the value of Δ_p for Mo isotopes seems to be too small, other values are nearly equal to values¹³ used usually. We have adopted the smoothing method with a 1.0 MeV width for comparison between calculated and exper-

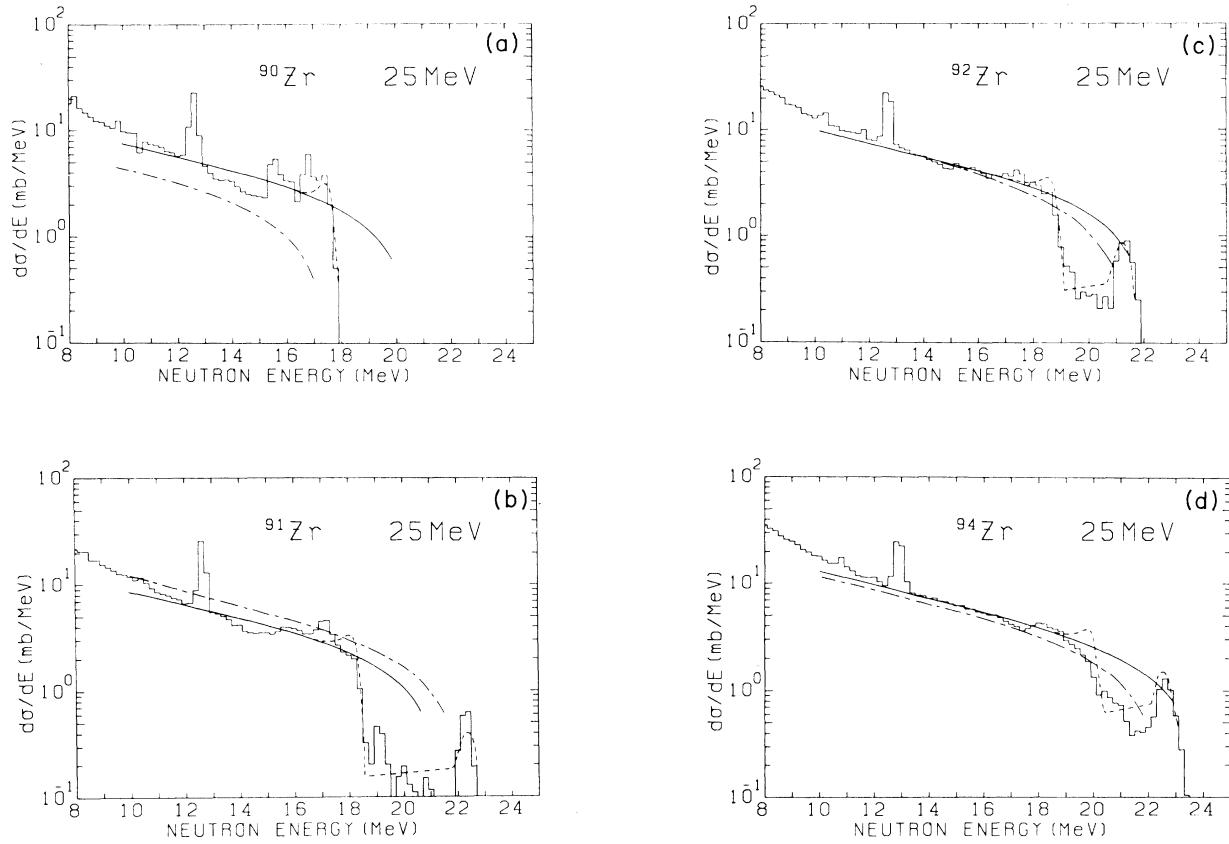


FIG. 4. Calculated and experimental angle-integrated energy spectra of neutrons for 25 MeV (p,n) reaction on Zr isotopes. [Histograms: experimental spectra, dotted-dashed curves: uniform spacing (US) model using true Q values, solid curves: US model using effective Q values (Q_e), and dashed curves: modified uniform spacing model using Q_e plus pairing correlation.]

imental results. The choice of the width was made rather arbitrarily so as to give similar peak width to the experimental peak width near the ground states of the residual nuclei, although the width should actually increase with increasing excitation energy because of the fragmentation¹⁴ of the deep hole state. The energy spectra calculated using the effective Q values, the modified uniform spacing model, and the pairing correlation are shown by the dashed curves in Fig. 4.

The Fermi energy λ_p in Eq. (8) was chosen to be the energy of the lowest unoccupied state for proton particle states. For the neutron hole states to which the modified uniform spacing model was applied, λ_n was chosen to be the energy of the corresponding highest occupied state in the uniform spacing model, because the Fermi energy λ should be a smooth function of mass number and is free from fluctuations near closed shells. Thus if the modified uniform spacing model is used, as origin F (a fictitious ground state) for the calculated excited states corresponds naturally to the effective Q values which is shell independent; namely the origin F is shifted by $Q_e - Q_t$ from the true ground state.

The energy spectra calculated using the modified uniform spacing model and the pairing correlation were normalized in the low energy region ($E_n < 17$ MeV) so as to

fit the solid curves calculated using the effective Q value and the uniform spacing model. As is seen in Fig. 4, the calculated spectra show good agreement with the experimental ones, not only on the absolute cross sections in the energy region of $E_n = 12$ –18 MeV, but also on the observed spectra with pronounced structures in the energy region of $E_n > 18$ MeV.

Similar results were also obtained for Mo isotopes as can be seen in Fig. 5, where the K value was chosen to be 360 MeV^3 so as to obtain the overall good agreement with the experimental spectra. Figure 6 shows similar results for ^{110}Pd which is far apart from the magic number, where the uniform spacing model was used for both proton and neutron shell. Similar results were also obtained for Zr isotopes for 18 MeV protons as is seen in Fig. 7, where the K value was chosen to be 305 MeV^3 so as to obtain the overall good fit. The incident-energy dependence on the K value is seen in the (p,n) reaction. Thus the experimental energy spectra were reproduced very well by the preequilibrium calculation using the effective Q values, the modified uniform spacing model, and the pairing correlation.

In the present analysis, the deformation effect¹ was not taken into account. From the Nilsson model it is predicted that nuclear deformation leads to a decrease in the

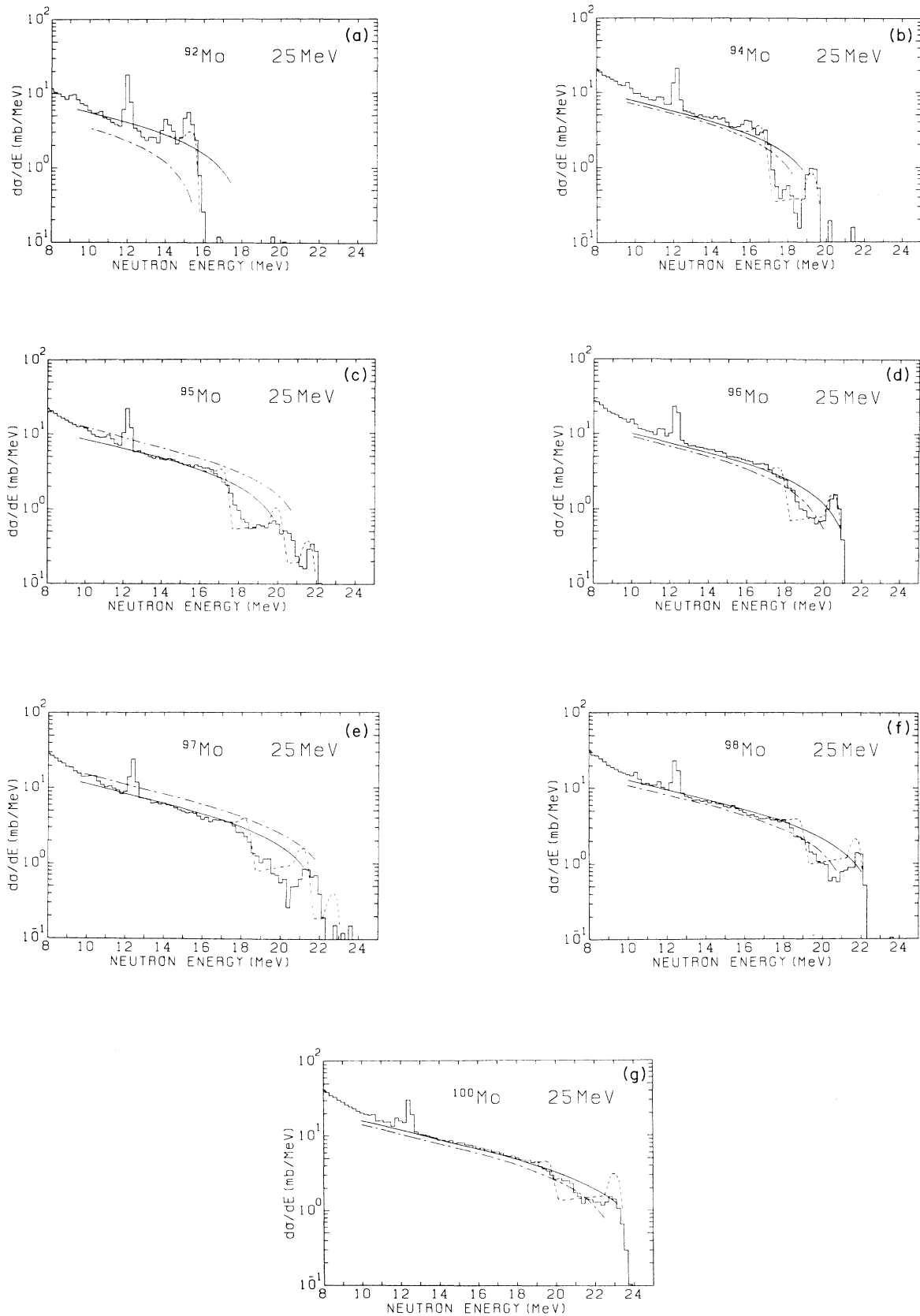


FIG. 5. Calculated and experimental angle-integrated energy spectra of neutrons for 25 MeV (p,n) reaction on Mo isotopes. See also the caption of Fig. 4.

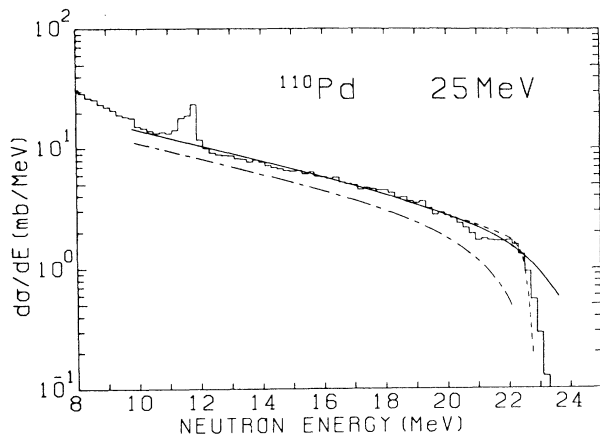


FIG. 6. Calculated and experimental angle-integrated energy spectra of neutrons for 25 MeV (p,n) reaction on ^{110}Pd . (Dotted-dashed curves: true Q value, solid curve: effective Q value, and dashed curve: effective Q value plus pairing correlation.)

$1g_{9/2}-2d_{5/2}$ energy difference and single particle level bunching. This implies that the modified shell model could approach to the uniform spacing model for the deformed nuclei (i.e., ^{100}Mo). Therefore if this effect is taken into account, the calculated spectra are expected to give better agreement with the experimental spectra by giving

duller structures for ^{94}Zr and $^{98,100}\text{Mo}$ around $E_n=18$ MeV with increasing mass number.

As shown in Figs. 4, 5, and 7, the experimental energy spectra for both the even-even nuclei and odd-mass nuclei are reproduced well by the calculated ones using the effective Q value, which is expressed by a smooth function of mass number and atomic number and has no odd-even effect in the energy spectra. From this fact it can be said that there exists no appreciable odd-even effect on the target nucleus for the preequilibrium (p,n) reaction, except for the spectra corresponding to the low lying states of the residual nuclei. When there is no appreciable odd-even difference in the energy spectra, we define it as "no odd-even effect." Of course, in this case there is odd-even effects for level densities corresponding to energy spectra measured from the ground states of the residual nuclei because of the difference of the true Q values. Thus it can be said that the experimental neutron energy spectra lower than 18 MeV with 25 MeV incident protons show no appreciable shell and odd-even effects in the preequilibrium process.

Recently, the authors and others¹⁵ have analyzed the energy spectra of the α particle emitted from the (p, α) reaction on isotopes of Mo with 15 and 18 MeV protons in terms of the preequilibrium exciton model using the effective Q value and the modified uniform spacing model similar to the present model. The shell effect of the gross structure of the energy spectra for nuclei near the magic

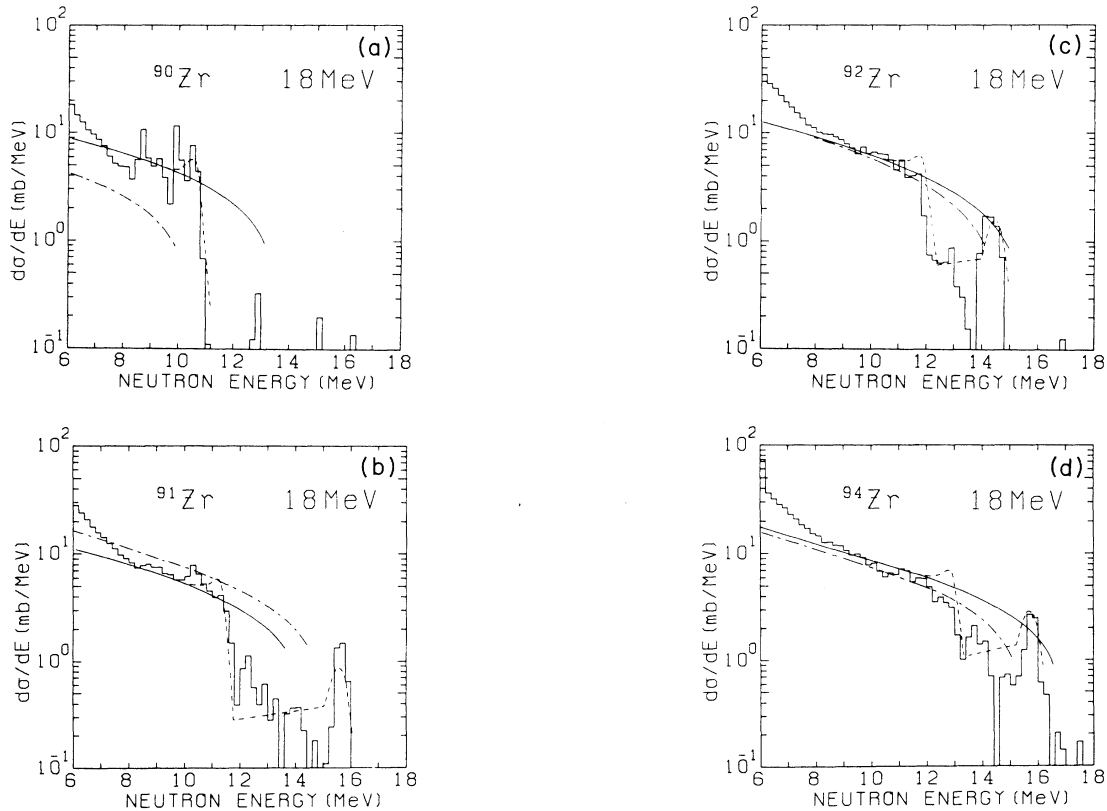


FIG. 7. Calculated and experimental angle-integrated energy spectra of neutrons for 18 MeV (p,n) reaction on Zr isotopes. See also the caption of Fig. 4.

nuclei can be explained very well in the model mentioned above.

The preequilibrium exciton model using the effective Q value, the modified uniform spacing model, and the pairing correlation would be applicable to the analysis of the 14 MeV (n,p) reaction which is the inverse reaction of the (p,n) reaction. The preliminary analysis of the experimental proton energy spectra emitted from 14 MeV (n,p) reaction on Mo isotopes has been performed using this model, and the calculated spectra show fairly good agreement with the experimental ones.

Fu¹⁶ proposed the advanced pairing correction $P(U,n)$ in which pairing gap $\Delta(U,n)$ depending on excitation U and exciton number n is employed in place of constant energy shift, as one of the methods including the pairing correction in the state density formula⁴ based on the uniform spacing model. From inspection of $\Delta(U,n)$, it is found that the calculated cross sections by Fu's method show almost the same values as those by the use of constant energy shift, if preequilibrium emission from $n=3$ states is dominant. This situation is applicable to the present analysis of neutron spectra in the energy region of more than 12 MeV using the effective Q value and the uniform spacing model. The use of the effective Q value Q_e corresponds to a constant energy shift $\Delta_{\text{eff}}=Q_t-Q_e$, where Q_t is the true Q value. Note that the value Δ_{eff} itself also contains the shell correction.

Recently, Mordhorst *et al.*¹⁷ have measured the differential cross sections for the ^{92,94,95,96,97,98,100}Mo (p,n) reaction with $E_p=25.6$ MeV. They have shown that angle integrated energy spectra show a clear odd-even pat-

tern if compared to two or more mass units away from the shell closure $N=50$. The pairing energies Δ necessary for their description in the framework of the geometry dependent hybrid model are larger than those in use for equilibrated systems. They can be correlated with a nuclear deformation parameter δ necessary to generate Δ from a set of realistic Nilsson model single particle states for the particle state density $\rho_{1,1}$ in the leading term of the preequilibrium model.

IV. CONCLUSIONS

The energy spectra for isotopes of Zr and Mo calculated using the effective Q value and the uniform spacing model show good agreement with the experimental ones except for $E_n > 18$ MeV. The analysis in terms of the preequilibrium exciton model using the effective Q value, the pairing correlation, and the modified uniform spacing model in which the uniform spacing model was modified so as to have wide spacing at the magic number was proposed. The calculated spectra by this method for the reaction on Zr and Mo isotopes with 25 MeV protons show good agreement with the experimental ones not only on the absolute cross sections in the neutron energy region of 12–18 MeV but also on the observed spectra with pronounced structures in the energy region higher than 18 MeV. Similar results were also obtained for Zr isotopes with 18 MeV incident protons. This model would be applicable to the analysis of 14 MeV (n,p) reaction which is the inverse reaction of the (p,n) reaction.

¹W. Scobel, M. Blann, T. T. Komoto, M. Trabant, S. M. Grimes, L. F. Hansen, C. Wong, and B. A. Pohl, *Phys. Rev. C* **30**, 1480 (1984).

²W. Scobel, M. Blann, T. T. Komoto, M. Trabant, S. M. Grimes, L. F. Hansen, C. Wong, and B. A. Pohl, Lawrence Livermore National Laboratory Report No. UCID-20101, 1984 (unpublished).

³F. C. Williams, Jr., A. Mignerey, and M. Blann, *Nucl. Phys.* **A207**, 619 (1973).

⁴F. C. Williams, Jr., *Phys. Lett.* **31B**, 184 (1970).

⁵I. Kumabe, *J. Nucl. Sci. Technol.* **18**, 563 (1981).

⁶G. M. Braga-Marcuzzan, E. Gadioli-Erba, L. Milazzo-Colli, and P. G. Sona, *Phys. Rev. C* **6**, 1398 (1972).

⁷A. H. Wapstra and K. Bos, *At. Data Nucl. Data Table* **19**, 215 (1977).

⁸A. Bohr and B. R. Mottelson, *Nuclear Structure* (Benjamin, New York, 1975), Vol. II, p. 649.

⁹J. M. Akkermans and H. Gruppelaar, Netherlands Energy

Research Foundation Report No. ECN-60, 1979; J. M. Akkermans, H. Gruppelaar, and G. Reffo, *Phys. Rev. C* **22**, 73 (1980).

¹⁰G. S. Mani, M. A. Melkanoff, and I. Iori, Centre a l'Energie Atomique Report No. CEA 2379 (unpublished).

¹¹A. Lindner, Institute für Kernphysik-Frankfurt Report No. EANDC(E)73 U, 1966 (unpublished).

¹²C. Kalbach-Cline, *Nucl. Phys.* **A210**, 590 (1973).

¹³A. G. W. Cameron and R. M. Elkin, *Can. J. Phys.* **43**, 1288 (1965).

¹⁴G. F. Bertsch, P. F. Bortignon, and R. A. Broglia, *Rev. Mod. Phys.* **55**, 287 (1983).

¹⁵I. Kumabe, Y. Mito, M. Hyakutake, N. Koori, H. Sakai, and Y. Watanabe, *Phys. Rev. C* **35**, 467 (1987).

¹⁶C. Y. Fu, *Nucl. Sci. Eng.* **86**, 344 (1984).

¹⁷E. Mordhorst, M. Trabant, A. Kaminsky, H. Krause, and W. Scobel, *Phys. Rev. C* **34**, 103 (1986).